AMERICAN SOCIETY FOR MICROBIOLOGY | Microbiology Spectrum

| Environmental Microbiology | Research Article

White-nose syndrome restructures bat skin microbiomes

Meghan Ange-Stark,[1] Katy L. Parise,[1,2] Tina L. Cheng,[3,4] Joseph R. Hoyt,[5] Kate E. Langwig,[5] Winifred F. Frick,[3,4] A. Marm Kilpatrick,[3] John Gillece,[2] Matthew D. MacManes,[1] Jeffrey T. Foster[1,2]

AUTHOR AFFILIATIONS See affiliation list on p. 12.

ABSTRACT The skin microbiome is an essential line of host defense against pathogens, yet our understanding of microbial communities and how they change when hosts become infected is limited. We investigated skin microbial composition in three North American bat species (*Myotis lucifugus*, *Eptesicus fuscus*, and *Perimyotis subflavus*) that have been impacted by the infectious disease, white-nose syndrome, caused by an invasive fungal pathogen, *Pseudogymnoascus destructans*. We compared bacterial and fungal composition from 154 skin swab samples and 70 environmental samples using a targeted 16S rRNA and internal transcribed spacer amplicon approach. We found that for *M. lucifugus*, a species that experiences high mortality from white-nose syndrome, bacterial microbiome diversity was dramatically lower when *P. destructans* was present. Key bacterial families—including those potentially involved in pathogen defense—significantly differed in abundance in bats infected with *P. destructans* compared to uninfected bats. However, skin bacterial diversity was not lower in *E. fuscus* or *P. subflavus* when *P. destructans* was present despite populations of the latter species declining sharply from white-nose syndrome. The fungal species present on bats substantially overlapped with the fungal taxa present in the environment at the site where the bat was sampled, but fungal community composition was unaffected by the presence of *P. destructans* for any of the three bat species. This species-specific alteration in bat skin bacterial microbiomes after pathogen invasion may suggest a mechanism for the severity of white-nose syndrome in *M. lucifugus* but not for other bat species impacted by the disease.

IMPORTANCE Inherent complexities in the composition of microbiomes can often preclude investigations of microbe-associated diseases. Instead of single organisms being associated with disease, community characteristics may be more relevant. Longitudinal microbiome studies of the same individual bats as pathogens arrive and infect a population are the ideal experiment but remain logistically challenging; therefore, investigations like our approach that are able to correlate invasive pathogens to alterations within a microbiome may be the next best alternative. The results of this study potentially suggest that microbiome-host interactions may determine the likelihood of infection. However, the contrasting relationship between Pd and the bacterial microbiomes of *Myotis lucifugus* and *Perimyotis subflavus* indicate that we are just beginning to understand how the bat microbiome interacts with a fungal invader such as Pd.

KEYWORDS bat populations, disease ecology, microbiome, *Myotis lucifugus*, *Perimyotis subflavus*, *Eptesicus fuscus*, *Pseudogymnoascus destructans*, white-nose syndrome

The microbiome is defined as the collection of microbes (composed of bacteria, fungi, protozoa, and viruses) that live in and on an organism (1). Microbiomes are increasingly being recognized as critical components of host health, directly influencing a range of biochemical and physiological processes (2). For mammalian

Editor Xia Ding, College of Life Sciences, Nanchang University, Nanchang, Jiangxi, China

Address correspondence to Meghan Ange-Stark, meghanange@gmail.com.

The authors declare no conflict of interest.

Received 30 June 2023
Accepted 13 September 2023
Published 27 October 2023

skin microbiomes in particular, specific taxa are recognized as common inhabitants, although these communities are just beginning to be characterized (3). Researchers have identified several bacterial species that are associated with skin disease in humans (4–6), including *Staphylococcus aureus*, which is linked to atopic dermatitis in children (7), *Corynebacterium minutissimum*, the agent of erythrasma, a chronic, superficial infection that causes lesions, and *Streptococcus pyogenes*, the most common agent of cellulitis, a diffuse inflammation of loose connective tissue (8). In wildlife, a fungal pathogen, *Batrachochytrium dendrobatidis*, the causative agent of chytridiomycosis in the skin of amphibians, has devastated amphibian populations worldwide (9–11). However, many species of bacteria exist as commensals and confer benefits to their hosts, including defense against pathogens and aiding in metabolism and reproduction (2). Examples include various staphylococcal species that inhibit skin inflammation after injury (12), as well as *Staphylococcus epidermidis*, which has been known to protect humans from an array of pathogenic bacteria such as *S. aureus*. Likewise, cutaneous microbes on amphibians might even play a protective role, allowing for resistance to pathogenic fungi (13–16).

While numerous microbiome studies have been conducted for wildlife diseases and correlations between pathogen colonization and microbial diversity have been observed, determining causality remains challenging. Previous studies have shown that pathogens can alter the microbiome. For example, *B. dendrobatidis* (Bd) disturbs the frog skin microbiome during both natural and experimental infection; bacterial richness was significantly lower in Bd-infected frogs compared with uninfected frogs (17, 18). Similarly, snake fungal disease was correlated with a reduction in bacterial and fungal diversity in an endangered rattlesnake (19). In Sea Star Wasting Disease, changes in microbial community composition occur during disease progression, with decreasing species richness in the late stages of the disease (20). With such perturbations to microbiomes following the introduction of various pathogens, continued investigation of skin microbial inhabitants—both pathogens and commensals—is crucial to understanding microbial pathogenesis and the role of the microbiome in animal health.

White-nose syndrome (WNS) in bats, caused by the fungal pathogen *Pseudogymnoascus destructans* (Pd), has become another prominent example of a lethal skin infection in wildlife (21–23). WNS is characterized by cutaneous infection during hibernation (24). The onset and growth of Pd on bat skin cause dehydration, fat loss, and electrolyte imbalance that disrupts bats' natural torpor cycle resulting in the depletion of fat reserves and mortality (25, 26). WNS emerged in North American bats in winter 2005/2006 (21–23) and has caused massive declines in bat populations throughout its spread across the Northeast and Midwestern US and Eastern Canada (27–31) Population declines at hibernating sites have been severe, leading to local extirpation of some species (28, 29), and much smaller persisting populations of other species (30, 32, 33). Once surviving bats leave hibernacula, increases in body temperature and restored immune function enable bats to clear infection (34, 35). However, Pd conidia remaining in caves can persist in the absence of bats, resulting in reinfection the following winter (34, 36, 37). Mortality rates from WNS vary among bat species (29, 38, 39), and environmental conditions of hibernacula may be strong predictors of species impacts (39). However, additional variation that could not be explained by environmental conditions alone suggests that interactions with other processes (e.g., behavioral, immune response, and microbiomes) may play a role in WNS susceptibility (39). While investigations into the microbiomes of North American bats have been conducted to help characterize their skin microbiota (40–45), host-microbial interactions and their impact on bat health remain an important knowledge gap (40). Comparing the bacterial and fungal microbial composition of Pd-positive and Pd-negative bats across the range of Pd spread in North America provides an opportunity to investigate the changes a pathogenic fungus has on the host skin microbial community across several bat species. In addition, distinguishing resident bat skin microbiota from microbiota found in the surrounding environment can

further contribute to our understanding of how host skin microbiomes are shaped by and interact with local microbiota (46).

We examined the epidermal microbiomes of three North American bat species: *Myotis lucifugus*, *Perimyotis subflavus*, and *Eptesicus fuscus*. These species were selected because they differ in both sociality and susceptibility to WNS and have been well sampled across a broad range. Both *M. lucifugus* and *P. subflavus* are heavily impacted by WNS (28, 29, 32), while *E. fuscus* is much less affected, (29, 39). We used a targeted 16S rRNA and internal transcribed spacer (ITS) amplicon approach comparing Pd-positive and Pd-negative bat skin swabs to examine interactions between bat epidermal bacterial and fungal microbiomes. We also classified the resident and transient microbes by comparing bat skin swabs to environmental (substrate) swabs to determine which members of the microbiome potentially serve as commensals and which may be transients from the environment. We hypothesized that bats infected with Pd will have lower skin microbial diversity but only for species that are heavily impacted by WNS (*M. lucifugus* and *P. subflavus*; not *E. fuscus*), and bacterial species that occur in higher abundance on Pd-positive bats will enhance anti-fungal properties in the microbial communities. Additionally, we predicted that we would find a significant difference in the microbiome composition between bat skin swabs and environmental swabs because only a fraction of bacteria and fungi in the environment may be able to colonize bats' skin.

MATERIALS AND METHODS

Data collection

Three species of hibernating bats (*E. fuscus*, big brown bat; *P. subflavus*, tri-colored bat; and *M. lucifugus*, little brown bat) were sampled throughout the eastern U.S. (Fig. 1). Samples were collected as part of a larger effort to track and document the spread of Pd using epidermal swabbing of bats during winter hibernacula surveys conducted over six consecutive winters from 2009/2010 to 2015/2016. A complete list of samples, their collection sites, and dates is available in the supplemental materials section (Table S1). Participating biologists were provided a detailed sampling protocol and video instructions to standardize sampling across sites and years (32). Epidermal swab samples were collected by dipping a sterile polyester swab in sterile water and rubbing the swab five times over the bat's forearm and muzzle (34). Substrate swab samples were simultaneously collected from the ceiling or walls of each hibernaculum at least 10 cm from a roosting bat. After collection, swabs were placed in vials containing RNAlater (Thermo Fisher Scientific, Waltham, MA) and were subsequently stored at −20°C, until DNA extraction.

DNA extraction and testing

Bat and substrate swabs were extracted using DNeasy Blood and Tissue extraction kits (Qiagen, Valencia, CA). The protocol was modified to include lyticase during the lysis step in addition to the proteinase K and buffer ATL as a way to enhance Pd extraction (47). Both the bacterial and fungal amplifications used this same extraction. Pd DNA quantity for each sample was tested using a quantitative PCR assay (48). Pd load was calculated based on a serial dilution of *P. destructans* isolate 20,631–21 and the equation detailed in Janicki et al. (49). Samples were run in duplicate, with 16 negative control wells distributed across each plate to detect potential contamination, which was not detected in any of the plates used in this work. Samples were considered Pd-positive if at least one of two qPCR cycle thresholds (Ct) was below 40. Pd loads were averaged when both replicates were positive. Additional details of the extraction and qPCR process are given in Huebschman et al. (50).

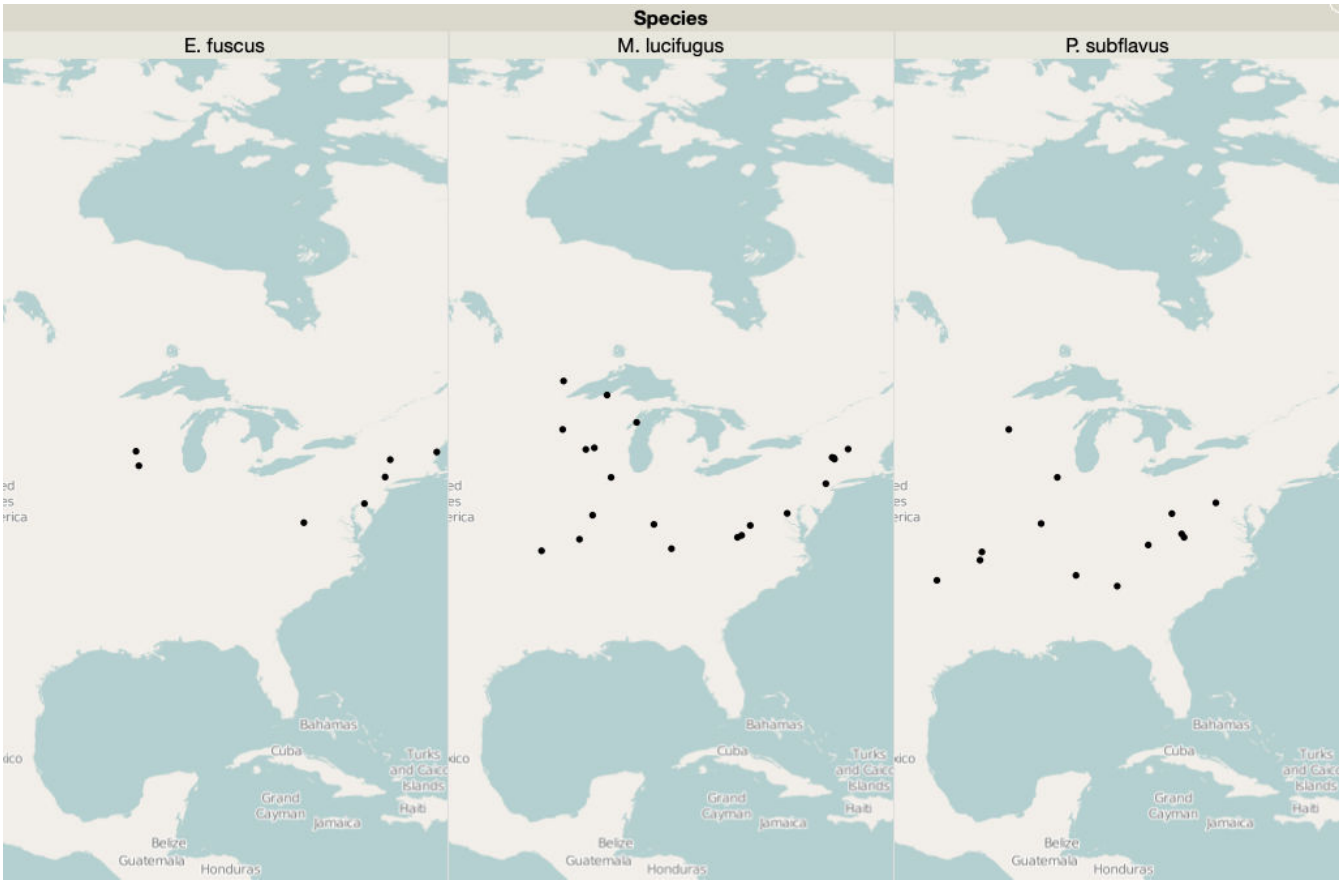

FIG 1 Bat sample collection distribution map. *E. fuscus* samples were collected from seven hibernacula 2011–2015. *M. lucifugus* samples were collected from 20 hibernacula 2011–2016. *P. subflavus* samples were collected from 13 hibernacula 2011–2016.

Amplification and sequencing

The DNA extracted from samples was prepped for sequencing following the Earth Microbiome Project 16S Illumina Amplicon Protocol and ITS Illumina Amplicon Protocol [earthmicrobiome.org; (51)] to test for bacterial and fungal taxa, respectively. Completed 16S rRNA and ITS libraries were submitted for 2 × 250 bp paired-end sequencing on a HiSeq 2500 at the University of New Hampshire's Hubbard Center for Genome Studies.

16S rRNA libraries were prepared by first amplifying the hypervariable region V4 of the 16S small subunit ribosomal gene with forward (barcoded) primer 515FB and reverse primer 806RB and an annealing temperature of 50°C for 60 s. Negative controls were included during amplification to account for possible contamination. Amplicons from each sample were run on an agarose gel to verify the presence of PCR product, with an expected band size for 515f–806r of ~300–350 bp. Amplicons were then quantified via a Qubit fluorometer (Thermo Fisher Scientific). An equal amount of amplicon from each sample (240 ng) was combined into a single, sterile tube. Amplicon pools were then cleaned using a QIAquick PCR Purification Kit (Qiagen), following the manufacturer's instructions. An aliquot of the final pool was submitted for sequencing with the 16S rRNA forward and reverse sequencing primers as well as the index sequencing primer.

ITS libraries were prepared by first amplifying the nuclear ribosomal ITS region with the forward primer ITS1f and reverse (barcoded) primer ITS2 using an annealing temperature of 52°C for 30 s. Negative controls were included during amplification to account for possible contamination. Amplicons from each sample were run on an agarose gel to verify the presence of PCR product, with an expected band size for ITS1f–ITS2 of ~230 bp. Amplicon cleanup and pooling followed the procedures detailed above for 16S rRNA libraries.

Data processing

Adapter sequences were removed using cutadapt (52). Sequence quality control, feature table construction, and raw sequence merging were performed using DADA2 version 1.8 in QIIME 2 (https://qiime2.org/). Unpaired reads were removed from the data set. Feature tables for each sequence type contained counts (frequencies) of each unique sequence in each sample within the data set. Additionally, this step detected and corrected Illumina amplicon sequence data, while also filtering any phiX reads as well as chimeric sequences. Best practices for microbial community analyses require that contamination caused by reagents and laboratory steps be removed as their presence can critically impact sequence-based microbial analyses (53, 54). In our specific work, 16S sequence contamination present as a by-product of lyticase use during the DNA extraction step was detected in the negative controls and subsequently filtered out by removing reads corresponding to *Arthrobacter luteus* and related species (i.e., *Cellulosimicrobium* spp.) from the entire 16S data set. Common reagents and laboratory contaminants found in the negative controls (e.g., *Pseudomonas* and *Sphingomonas*) were also filtered out by removing corresponding reads. Additionally, taxa that accounted for less than 0.1% of the total read sets were removed from each of the respective data sets before downstream analyses.

In order to conduct diversity analyses, a multiple sequence alignment was constructed to create an aligned sequences feature table using mafft version 7.407 [https://mafft.cbrc.jp/alignment/software/; (55)]. Highly variable positions were removed to reduce noise in the phylogenetic tree. FastTree version 2.1 [http://www.microbesonline.org/fasttree/;(56)] was applied to the filtered alignment, creating an unrooted phylogenetic tree where midpoint rooting was done at the midpoint of the longest tip-to-tip distance to create a rooted tree.

Microbial diversity analyses

QIIME2 version 2018.2 was used to conduct diversity analyses with accompanying statistical tests. The core metrics phylogenetic method computed and provided interactive visualizations for alpha and beta diversity metrics, while also generating principal coordinate analysis (PCoA) plots using Emperor (https://biocore.github.io/emperor/) for beta diversity analyses. 16S read counts were rarefied to 4,160 reads per sample, and ITS read counts were rarefied to 6,167 reads per sample in order to retain as many samples as possible while also accounting for the amount of coverage needed to calculate meaningful diversity metrics. Alpha rarefaction plots indicated no increase in the number of bacterial or fungal operational taxonomic units (OTUs) with increased sequencing depth when rarefied to 4,160 and 6,167 reads per sample, respectively (Fig. S1).

Associations between categorical metadata (Pd infection status, sample type, phylogeny, etc.) and alpha diversity data were conducted to determine any significant differences between metadata groups in QIIME2. Likewise, sample composition in the context of categorial metadata using beta diversity metrics was analyzed using PERMANOVA (57). These tests determined which specific pairs of metadata groups differed from one another.

Linear mixed-effects modeling analyses

To better understand the variables potentially driving skin bacterial diversity differences between Pd-positive and Pd-negative bats, we fit a linear mixed-effects model that included Pd presence (coded as 0/1), site latitude, site longitude, and monthly average outside temperature of sample collection site as fixed effects and sample collection site and sample date as random effects to account for multiple bats sampled at each site as well as inter-year variation. Pd presence was determined using quantitative PCR (48) as described above. Monthly average temperatures of the sample collection date were collected from the National Oceanic and Atmospheric Association Climate Database

(https://www.ncdc.noaa.gov/). Latitude at the sample collection site was included as a covariate to account for potential latitudinal diversity gradients in terrestrial bacteria (58), while winter/early spring sample selection was done to account for seasonal effects on microbial composition. Models were fit using the lmer function in the R package lme4. We assumed a Gaussian distribution and checked model residuals to confirm normality for each response variable (richness, evenness, and Shannon index) for each species.

Taxonomic identification and differential abundance analyses

Identifying the taxonomic composition of 16S rRNA sequences required the use of a pre-trained Naive Bayes classifier as well as the QIIME2 feature classifier plugin, which was trained on the Greengenes 13_8 99% OTUs, where the sequences have been trimmed to only include 250 bases from the region of the 16S rRNA that was sequenced in the analysis (the V4 region, bound by the 515F/806R pair). ITS taxonomic identification leveraged the UNITE database version 7.2 (https://unite.ut.ee/). The linear discriminant analysis effect size (LEfSe) was used to conduct microbial differential abundance analyses [http://huttenhower.sph.harvard.edu/lefse/; (59)].

RESULTS

For bacteria, 93,382,083 16S rRNA sequences were amplified in 224 samples with a mean frequency of 413,195 reads per sample. Of those 224 samples, 154 were bat skin swabs, and the remaining 70 were substrate swabs. After filtering the total read set for *Cellulosimicrobium*, the 16S data set was reduced to 3,694,218 sequences with a mean frequency of 16,492 sequences per sample. Rarefaction of the 16S data (Fig. S1A) indicated a read minimum of 4,160 reads per sample for downstream analyses, reducing the total number of bacterial samples for analysis to 132:70 bat skin swabs and 62 substrate swabs. For fungi, 17,251,679 ITS sequences were amplified from 498 samples. Of those 498 samples, 375 samples were bat skin swabs, and the remaining 123 were substrate swabs. A mean of 34,503 sequences were obtained per bat skin sample. Rarefaction of the ITS data set (Fig. S1B) indicated a read minimum of 6,167 reads per sample for downstream analyses, reducing the total number of fungal samples to 251:158 bat skin swabs and 93 substrate swabs.

Bacterial and fungal skin microbiome dissimilarities between Pd-negative bat species

Jaccard distance matrices that quantitatively measured bacterial community dissimilarity showed that when measuring bacterial species presence and absence among bat species, the skin of *E. fuscus* and *P. subflavus* were the most similar in bacterial community composition (Fig. S2 and S4, A; $P = 0.19$), while *P. subflavus* and *M. lucifugus* were the most dissimilar (Figs. S2 and S4, A, $P = 0.02$). Jaccard distance matrices for fungal community dissimilarity showed high levels of fungal community dissimilarity between all species pairs (Fig. S3 and S4, B; E. *fuscus* and *M. lucifugus*, $P = 0.001$; *E. fuscus* and *P. subflavus*, $P = 0.001$; *M. lucifugus* and *P. subflavus*, $P = 0.008$).

Characterization of Pd-negative bacterial and fungal microbiomes of three bat species

The bacterial (Fig. S5; Table S2) and fungal (Fig. S6; Table S2) skin microbiomes of Pd-negative *E. fuscus*, *M. lucifugus*, and *P. subflavus* were characterized to better understand the composition of skin microbiota without Pd present and to represent skin microbiomes before Pd invasion. These samples were all taken from bats from areas where WNS and Pd had not yet been detected (i.e., at least one year prior to known Pd arrival). *Pseudomonadales* and *Actinomycetales* were two of the most abundant bacterial orders across all three bat species, but the relative abundance and dominance of each order differed among bat species (Fig. 2). Bacterial communities on *E. fuscus* (Fig. 2, A1) were dominated by a single order (*Pseudomonadales*), whereas skin microbiomes

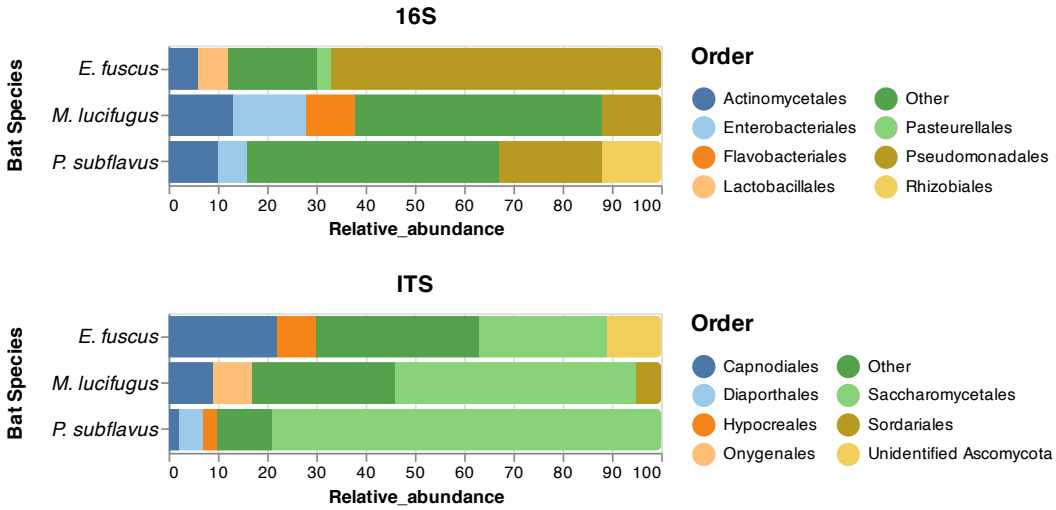

FIG 2 Bacterial and fungal microbiome taxonomy characterization. Bacterial characterization at the order level showed that for *E. fuscus* (A1) 66.5% of the bacterial OTUs were assigned to the order *Pseudomonadales*, for *M. lucifugus* (B1), *Enterobacteriales* was the most abundant bacterial order with 15.4% of the bacterial OTUs, and *Pseudomonadales* was the most abundant bacterial order for *P. subflavus* (C1) with 20.9% of the bacterial OTUs. Fungal microbiome characterization at the order level showed that for all three bat species, *Saccharomycetales* was the most abundant fungal order; however, it's abundance varied significantly between each species (*E. fuscus*, 25.6%; *M. lucifugus*, 49.4%; *P. subflavus*, 79.2%).

were much more even on *M. lucifugus* (Fig. 2, B1) and *P. subflavus* (Fig. 2, C1). *Pseudomonadales*, in fact, was the most common bacterial order for both *E. fuscus* (66.5% of OTUs) and *P. subflavus* (20.9%) and the third most common bacteria on *M. lucifugus* (12.3%). *Actinomycetales* was also a dominant order on all three species, making up 6.1%, 12.6%, and 9.9% of bacterial OTUs on *E. fuscus, M. lucifugus*, and *P. subflavus*, respectively.

Saccharomycetales was the most common fungal order across all three bat species; however, its relative abundance varied by bat species. *E. fuscus* (Fig. 2, A2) displayed higher levels of evenness with relatively similar abundances of *Saccharomycetales* and its second most abundant order, *Capnodiales*, while fungal communities on *M. lucifugus* (Fig. 2, B2) and *P. subflavus* (Fig. 2, C2) were both dominated by *Saccharomycetales*. *Capnodiales* and *Onygenales*—the second and third most abundant fungal orders for *M. lucifugus*—each made up less than 10% of its fungal microbiome. The same was true for *P. subflavus*, with *Diaporthales* and *Hypocreales* each making up less than 5% of the fungal microbiome as the second and third most abundant fungal orders.

Microbial diversity analyses: microbiome differences based on Pd presence

Species richness, evenness, and Shannon diversity were similar in Pd-positive and Pd-negative *E. fuscus* bat samples for both bacterial (Fig. 3, A1; Evenness: $\chi^2 = 0.47$, $P = 0.52$, Richness: $\chi^2 = 0.85$, $P = 0.92$, and Shannon Diversity: $\chi^2 = 0.72$, $P = 0.78$) and fungal microbiomes (Fig. 3, B1; Evenness: $\chi^2 = 0.10$, $P = 0.10$, Richness: $\chi^2 = 0.13$, $P = 0.13$, and Shannon Diversity: $\chi^2 = 0.09$, $P = 0.09$). Fungal communities for *M. lucifugus* were also similar in species diversity (Fig. 3, B2; Richness: $\chi^2 = 0.83$ $p = 0.84$, Shannon Diversity: $\chi^2 = 0.86$, $P = 0.86$) and evenness (Fig. 3, B2; $\chi^2 = 0.95$, $P = 0.96$) when comparing Pd-negative and positive samples. In contrast, bacterial microbiomes in *M. lucifugus* were less diverse (Fig. 3, A2; Richness: $\chi^2 = 0.33$, $P = 0.34$, Shannon Diversity: $\chi^2 = 0.01$, $P = 0.01$) due to reduced evenness (Fig. 3, A2; $\chi^2 = 0.003$, $P = 0.003$) in Pd-positive samples. Bacterial microbiomes for *P. subflavus* were similar between Pd-positive and negative bats (Fig. 3, A3; Evenness: $\chi^2 = 0.13$, $P = 0.14$, Richness: $\chi^2 = 0.68$, $P = 0.70$, and Shannon Diversity: $\chi^2 = 0.20$, $P = 0.21$), whereas fungal microbiomes had higher evenness (Fig. 3, B3; $\chi^2 = 0.001$, $P = 0.001$) and diversity (Fig. 3, B3; $\chi^2 = 0.003$, $P = 0.003$) in the Pd-positive group than the Pd-negative group but not in richness (Fig. 3, B3; $\chi^2 = 0.22$, $P = 0.22$). Thus, there appeared

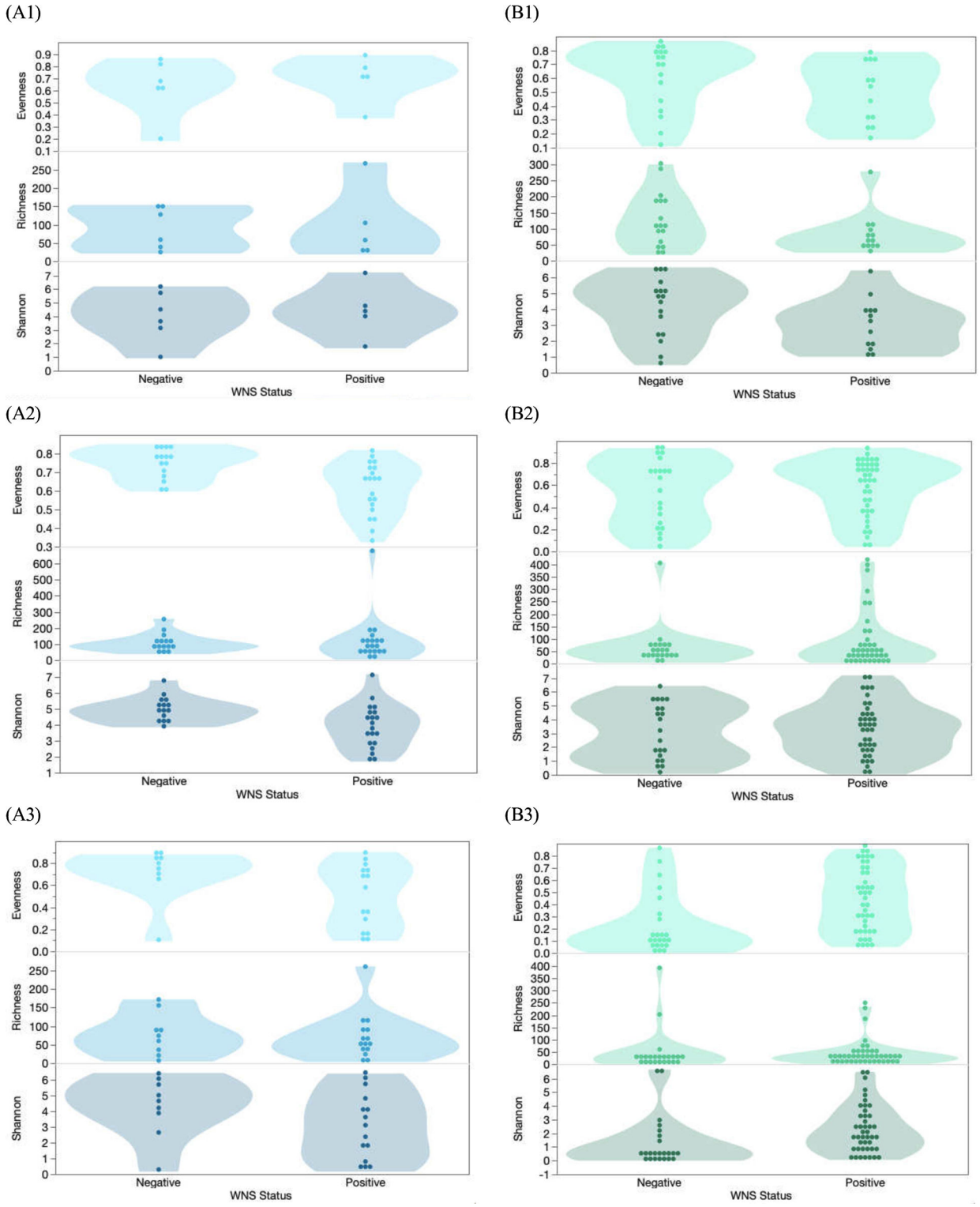

FIG 3 Measures of bacterial and fungal evenness, richness, and Shannon indices between Pd-positive and Pd-negative bats. There were no significant differences when comparing (A1) bacterial or (B1) fungal diversity between Pd-positive and Pd-negative *E. fuscus*. (A2) Bacterial diversity comparisons in *M. lucifugus* found the evenness, richness, and Shannon diversity were all significantly higher in Pd-negative bats. (B2) Fungal diversity comparisons in *M. lucifugus* did not indicate any difference between Pd-positive and Pd-negative bats. (A3) There were no significant differences when comparing bacterial diversity between Pd-positive and Pd-negative *P. subflavus*; however, (B3) fungal diversity results from *P. subflavus* indicate that Pd-positive bats have a higher fungal evenness and Shannon diversity.

to be substantial variation in the effects of the presence of Pd on bat microbiomes and that variation appears to differ by bat host.

Does Pd influence *M. lucifugus*' skin bacterial microbiome?

Fungal diversity for *M. lucifugus* was most influenced by both average temperature and latitude, as one or both of these covariates were significant for all three response variables (Richness: monthly average temperature, $P = 0.042$, PE = 1.4, SE = 0.66; Evenness: monthly average temperature, $P = 0.024$, PE = 0.008, SE = 0.003, and latitude, $P = 0.031$, PE = 0.03, SE = 0.01; Shannon Diversity: monthly average temperature, $P = 0.005$, PE = 0.07, SE = 0.02, and latitude, $P = 0.046$, PE = 0.18, SE = 0.24). In contrast, results for *P. subflavus* indicated that sample date most influenced fungal richness ($P = 0.01$, PE = 0.26, SE = 0.09) and Shannon diversity ($P = 0.042$, PE = 0.008, SE = 0.004) when compared to the other covariates. We found no clear effect of Pd presence, temperature, latitude, and sampling date on bacterial evenness or diversity for *P. subflavus* or *E. fuscus*; however, Pd presence (0/1) on *M. lucifugus* was associated with significantly decreased bacterial diversity (Evenness: $P = 0.012$, PE = 0.05, SE = 0.02; Shannon Diversity: $P = 0.001$, PE = 0.66, SE = 0.18). Increases in Pd load in a sample corresponded with decreased Shannon diversity in *M. lucifugus*, although the result was not statistically significant (Fig. S7).

Taxonomic differential abundance analyses in Pd-positive and Pd-negative *M. lucifugus*

Comparisons of skin microbial diversity between Pd-positive and Pd-negative *M. lucifugus* uncovered substantial differences in bacterial taxa between the two groups, as both evenness and Shannon diversity were significantly lower in the Pd-positive bats. A differential abundance analysis (Fig. 4) indicated that one family of bacteria, *Pseudonocardiaceae*, was overly abundant among Pd-positive *M. lucifugus*. Conversely, bacterial families *Brucellaceae*, *Cytophagaceae*, and *Rhizobiaceae*, as well as bacterial order *Chromatiales*, were abundant in Pd-negative *M. lucifugus*.

Comparison of skin microbiome between bats and substrates

Bacterial diversity was significantly higher on substrates than on bats (Fig. 5A, $\chi^2 = 0.0001$, $P < 0.001$), with 17 abundant bacterial families represented in the substrate samples and only four overly abundant bacterial families represented in bat samples (Fig. S8). Fungal communities between the two sample types, however, were similar in diversity (Fig. 5B, $\chi^2 = 0.345$, $P = 0.345$) and taxa, as fungal taxa abundance comparisons between bat and substrate samples resulted in only one fungal order, *Helotiales*, being more represented in substrate samples than on bats. This result was not caused by the presence of Pd but rather by other members of *Helotiales*, which are common fungi within cave communities.

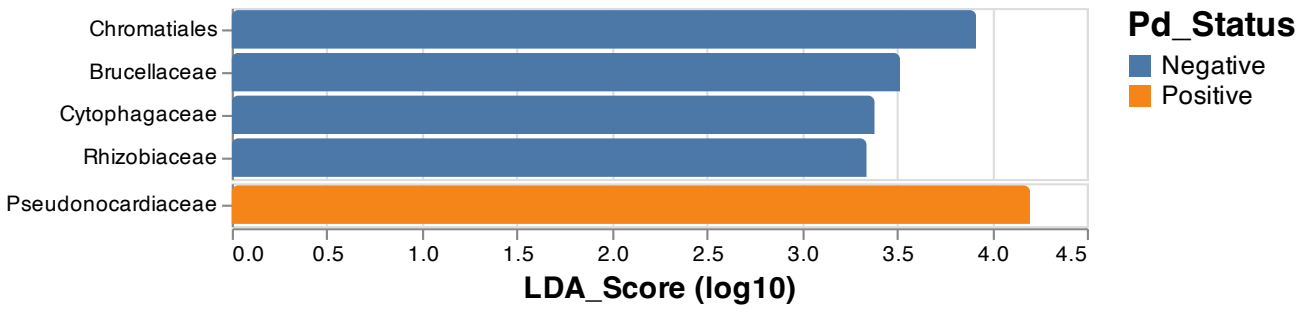

FIG 4 Relative abundances of bacterial epidermal communities of Pd-positive and Pd-negative *M. lucifugus*. Measures of relative abundance between the bacterial epidermal communities from swabs taken from Pd-positive and Pd-negative *M. lucifugus* revealed an overabundance of the bacterial family *Pseudonocardiaceae* in Pd-positive bats, while unaffected bats showed an overabundance of bacterial families *Brucellaceae*, *Cytophagaceae*, and *Rhizobiaceae*, as well as the bacterial order *Chromatiales*.

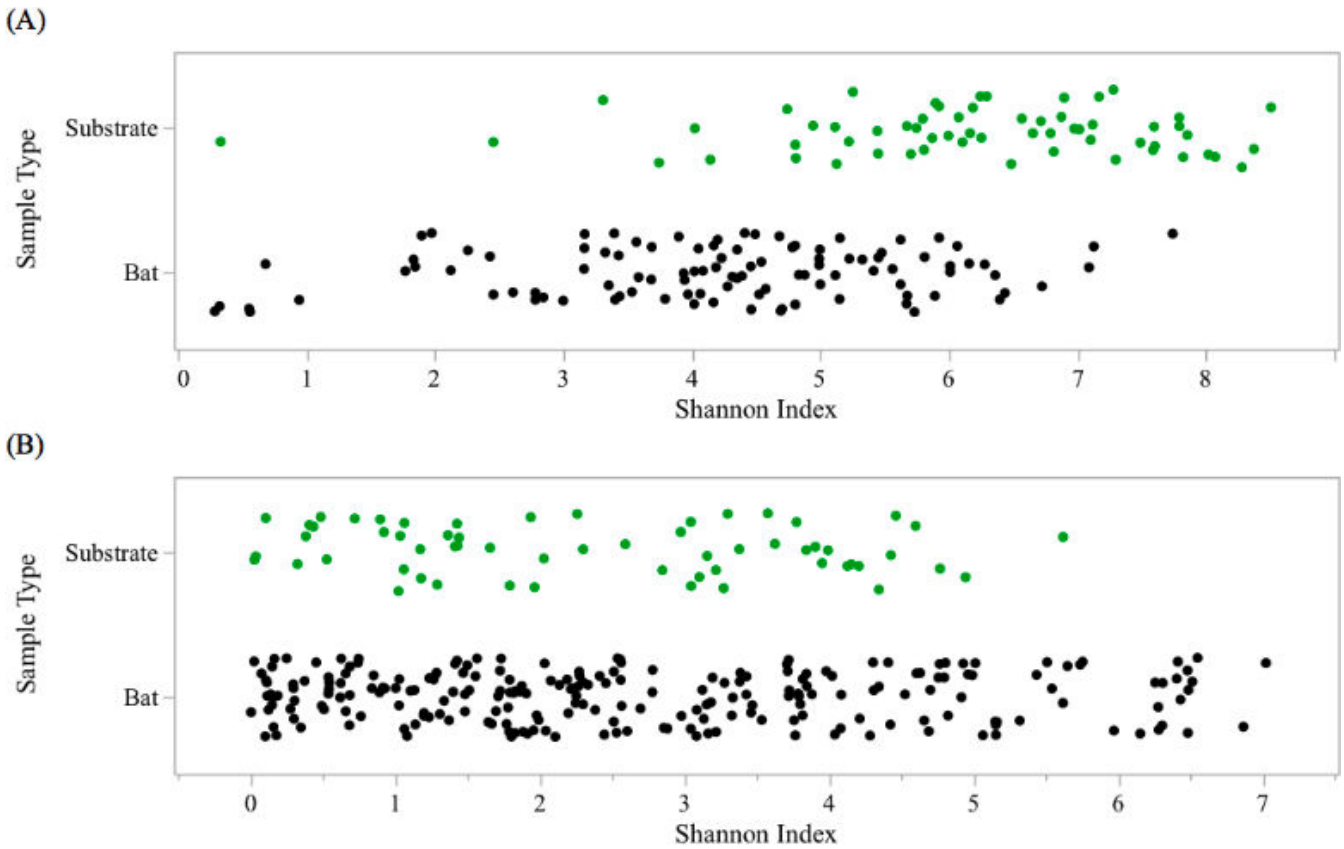

FIG 5 Bacterial (A) and fungal (B) differences between bat epidermal and substrate microbiome composition. Bacterial results indicate a significant difference in diversity between bat and substrate samples, with substrate samples containing a higher Shannon diversity. Fungal results did not indicate a significant difference in diversity between bat and substrate samples.

DISCUSSION

We found that one of the most heavily impacted bat species, *M. lucifugus*, which was once highly abundant but underwent massive die-offs from WNS (27), is also the bat species whose bacterial microbiome was most dramatically altered by the presence of Pd. Contrary to expectations, the bacterial microbiome does not appear to have a protective effect but rather appears affected by invasion and colonization by Pd, which suggests that Pd on these bats results in reductions in bacterial community diversity. This result was supported by the environmental modeling, which identified Pd presence as the only covariate significantly influencing all measures of bacterial diversity in *M. lucifugus*. Recent work on host-associated microbial community changes throughout the progression of Sea Star Wasting Disease also found community-wide differences in the microbiomes of affected and unaffected individuals, specifically noting a decrease in species richness of the microbiome in the late stages of the disease (20). Decreases in the diversity of host-associated microbial communities in other wildlife diseases (i.e., chytridiomycosis and snake fungal disease) have also occurred (13, 17–19).

When commensals decrease in abundance throughout the progression of disease, their reduced collective ability to perform functions that inhibit or prevent the growth of pathogens and/or opportunistic bacteria potentially leads to an increase in disease severity. If true, it is possible that Pd causes epidermal microbiome dysbiosis, where normally dominating species decrease in abundance, and to compensate, normally outcompeted/contained species increase in abundance. Alternatively, *M. lucifugus* with low bacterial richness and evenness may be more susceptible to colonization by Pd. Disentangling these competing hypotheses would require a longitudinal study in which

the microbiomes of the same individuals are assessed over time during Pd invasion, a data set that has proven to be logistically very difficult to acquire. However, our findings strongly suggest that Pd invasion can cause changes in bat skin microbiomes, and in fact, increases in Pd load are correlated with decreases in bacterial diversity.

A bacterial taxonomic differential abundance test between Pd-positive and Pd-negative *M. lucifugus* uncovered several bacterial taxa that are seemingly impacted by the onset and growth of Pd. The *Pseudonocardiaceae* family in the order *Actinomycetales* was significantly more abundant in Pd-positive bats, while bacterial order *Chromatiales* and bacterial families *Brucellaceae*, *Rhizobiaceae*, and *Cytophagaceae* were all significantly overrepresented in Pd-negative *M. lucifugus*. Investigations into the *Pseudonocardiaceae* family have found that certain members are involved in the production of antimicrobial agents under specific nitrogen conditions (60), with low nitrogen stimulating the production of antibacterial substances in the genera *Amycolatopsis*, *Saccharomonospora*, and *Saccharopolyspora* and high nitrogen stimulating the production of metabolites in the genus *Pseudonocardia*. Indeed, a well-studied and highly evolved mutualism between fungus-growing ants and their fungi has also uncovered antibiotic-producing bacteria within the *Pseudonocardiaceae* family (61). Attine ants and their fungi are mutually dependent, with the maintenance of stable fungal monocultures critical to the survival of both organisms. Examination of this symbiotic relationship found that attine ant fungal gardens also host a specialized and virulent parasitic fungus belonging to the genus *Escovopsis*, while filamentous bacterium from *Pseudonocardiaceae*—that are largely vertically transmitted between ant generations—produce antibiotics specifically targeted to suppress the growth of the specialized garden parasite (62, 63). This relationship in ants suggests a link between members of the *Pseudonocardiaceae* family and fungal pathogen defense, making its overrepresentation in Pd-positive bats intriguing as it points to potential host defense mechanisms.

As for bacterial orders overrepresented in Pd-negative *M. lucifugus*, a key characteristic of the *Cytophagaceae* family is that members of most species are able to degrade one or several kinds of organic macromolecules such as proteins (e.g., casein and gelatin), lipids, starches, and—most noteworthy in this case—chitin (64). Chitin, a long linear homopolymer of beta-1,4-linked N-acetylglucosamine, is a structurally important component of the fungal cell wall (65). In both yeasts and filamentous fungi, chitin microfibrils are formed from inter-chain hydrogen bonding. These polymers significantly contribute to the overall integrity of the cell wall, and when chitin synthesis is disrupted, the wall becomes disordered, and the fungal cell becomes malformed and osmotically unstable (65). Given this seemingly important bacterial family characteristic, its abundance in Pd-negative bats suggests a potential link between its enzymatic activity and its ability to limit Pd growth on bat skin—a finding supported by microbial isolates from Western Canadian bat wings (41). However, we note that this bacterial family was not common in *E. fuscus*, a bat species more tolerant to WNS.

While the *M. lucifugus* bacterial microbiome appeared to be affected by the presence of Pd, *E. fuscus* and *P. subflavus* bacterial microbiomes were similar between the Pd affected and unaffected groups—a finding further supported by a beta diversity study of Pd-inoculated *E. fuscus* bats that found that the most abundant bacterial taxa remained stable throughout the experiment (43). *E. fuscus* is one of the bat species least affected by WNS as they still rank among the most abundant and widespread bats in North America, even in regions where WNS has devastated populations of other bat species (30). In contrast, *P. subflavus* populations appear to be in rapid decline due to WNS (28, 29). Thus, it is curious that bacterial diversity in *P. subflavus* was not affected in the same manner as it was in *M. lucifugus*. One potential reason for the difference between *M. lucifugus* and *P. subflavus* has to do with their microbiomes prior to Pd infection. Beta-diversity analyses of Pd-negative *M. lucifugus* and *P. subflavus* (Fig. S3 and S5) indicate that their bacterial and fungal microbiomes were significantly different before the onset of disease, and this could potentially explain differences observed following Pd invasion. For fungal community composition, the presence of Pd did not impact fungal taxon richness or

evenness in *E. fuscus* or *M. lucifugus* but did impact the taxon evenness in *P. subflavus*, with significantly higher fungal community evenness in Pd-positive bats. Additionally, our findings suggest an influence of environment on the fungal species found on bats, as there were no significant differences in diversity or taxa between bat skin samples and the cave substrates, a pattern typically associated with transient (non-resident) members of a community (66, 67). Indeed, the fungal taxa present on bats appear to be a sample of what is present in the environment, with fungal spores adventitiously landing on bat skin rather than a commensal relationship of the fungi living on the host (68). Commensal fungi do occasionally grow on bats (69), but Pd appears to have adapted from an environmental microbe living in cave sediments to a pathogen that is able to utilize bat skin as a food source (70). Simply being a sampling of the environment was not the case for bacterial species, however, as there were significant differences in diversity between bats and substrates with substrate samples showing higher diversity. Additionally, relative abundance comparisons indicated overabundance in more than 20 bacterial families between bat and substrate samples. These results suggest that bat skin serves as a niche for certain bacterial species that remain as commensal members of the bat skin microbiome regardless of the environment. Moreover, these commensal bacteria on the bat do not appear to be readily shed into the environment even though the substrate samples were taken in close proximity to the bats.

Inherent complexities in the composition of the microbiome can often preclude investigations of microbe-associated diseases. Instead of single organisms being associated with disease, community characteristics (such as composition and metagenomic functionality) may be more relevant (2). Longitudinal microbiome studies of the same individual bats as Pd arrives and infects a population are the ideal experiment but remain logistically challenging; therefore, investigations like our approach that are able to correlate invasive pathogens to alterations within a microbiome may be the next best alternative. The results of this study potentially suggest that microbiome-host interactions may determine the likelihood of infection. However, the contrasting relationship between Pd and the bacterial microbiomes of *M. lucifugus* and *P. subflavus* indicate that we are just beginning to understand how the bat microbiome interacts with a fungal invader such as Pd.

AUTHOR AFFILIATIONS

[1]Department of Molecular, Cellular and Biomedical Sciences, University of New Hampshire, Durham, New Hampshire, USA
[2]Pathogen and Microbiome Institute, Northern Arizona University, Flagstaff, Arizona, USA
[3]Department of Ecology and Evolutionary Biology, University of California, Santa Cruz, California, USA
[4]Bat Conservation International, Austin, Texas, USA
[5]Department of Biological Sciences, Virginia Tech, Blacksburg, Virginia, USA

AUTHOR ORCIDs

Meghan Ange-Stark http://orcid.org/0000-0003-3231-9414
Kate E. Langwig http://orcid.org/0000-0001-8318-1238
Jeffrey T. Foster http://orcid.org/0000-0001-8235-8564

DATA AVAILABILITY

Raw sequencing reads are available at the NCBI Short Read Archive (accession number: PRJNA533244).

ADDITIONAL FILES

The following material is available online.

Supplemental Material

Figure S1 (Spectrum02715-23-s0001.pdf). 16S and ITS alpha rarefaction plots.
Figure S2 (Spectrum02715-23-s0002.pdf). 16S beta diversity analyses.
Figure S3 (Spectrum02715-23-s0003.pdf). ITS beta diversity analyses.
Figure S4 (Spectrum02715-23-s0004.pdf). 16S and ITS principal coordinate plots.
Figure S5 (Spectrum02715-23-s0005.pdf). 16S taxonomic bar plot.
Figure S6 (Spectrum02715-23-s0006.pdf). ITS taxonomic bar plot.
Figure S7 (Spectrum02715-23-s0007.pdf). Shannon diversity analysis.
Figure S8 (Spectrum02715-23-s0008.pdf). 16S differential abundance.
Table S1 (Spectrum02715-23-s0009.csv). Sample list.
Table S2 (Spectrum02715-23-s0010.csv). 16S and ITS orders per species.

REFERENCES

1. Turnbaugh PJ, Ley RE, Mahowald MA, Magrini V, Mardis ER, Gordon JI. 2006. An obesity-associated gut microbiome with increased capacity for energy harvest. Nature 444:1027–1031. https://doi.org/10.1038/nature05414
2. Cho I, Blaser MJ. 2012. The human microbiome: at the interface of health and disease. Nat Rev Genet 13:260–270. https://doi.org/10.1038/nrg3182
3. Ross AA, Müller KM, Weese JS, Neufeld JD. 2018. Comprehensive skin microbiome analysis reveals the uniqueness of human skin and evidence for phylosymbiosis within the class mammalia. Proc Natl Acad Sci U S A 115:E5786–E5795. https://doi.org/10.1073/pnas.1801302115
4. Findley K, Grice EA. 2014. The skin microbiome: a focus on pathogens and their association with skin disease. PLoS Pathog. 10:e1004436. https://doi.org/10.1371/journal.ppat.1004436
5. Kong HH, Oh J, Deming C, Conlan S, Grice EA, Beatson MA, Nomicos E, Polley EC, Komarow HD, Program NCS, Murray PR, Turner ML, Segre JA. 2012. Temporal shifts in the skin microbiome associated with disease flares and treatment in children with atopic dermatitis. Genome Res 22:850–859. https://doi.org/10.1101/gr.131029.111
6. Zeeuwen PLJM, Kleerebezem M, Timmerman HM, Schalkwijk J. 2013. Microbiome and skin diseases. Curr Opin Allergy Clin Immunol 13:514–520. https://doi.org/10.1097/ACI.0b013e328364ebeb
7. Kong HH. 2011. Skin microbiome: genomics-based insights into the diversity and role of skin microbes. Trends Mol Med 17:320–328. https://doi.org/10.1016/j.molmed.2011.01.013
8. Aly R. 1996. Microbial infections of skin and nails. In Medical Microbiology. University of Texas, Medical Branch at Galveston, Galveston (TX).
9. Berger L, Speare R, Daszak P, Green DE, Cunningham AA, Goggin CL, Slocombe R, Ragan MA, Hyatt AD, McDonald KR, Hines HB, Lips KR, Marantelli G, Parkes H. 1998. Chytridiomycosis causes amphibian mortality associated with population declines in the rain forests of Australia and Central America. Proc Natl Acad Sci U S A 95:9031–9036. https://doi.org/10.1073/pnas.95.15.9031
10. Longcore JE, Pessier AP, Nichols DK. 1999. *Batrachochytrium dendrobatidis* gen. et sp. nov., a chytrid pathogenic to amphibians. Mycologia 91:219–227. https://doi.org/10.1080/00275514.1999.12061011
11. Piotrowski JS, Annis SL, Longcore JE. 2004. Physiology of batrachochytrium dendrobatidis, a chytrid pathogen of amphibians. Mycologia 96:9–15.
12. Lai Y, Di Nardo A, Nakatsuji T, Leichtle A, Yang Y, Cogen AL, Wu Z-R, Hooper LV, Schmidt RR, von Aulock S, Radek KA, Huang C-M, Ryan AF, Gallo RL. 2009. Commensal bacteria regulate toll-like receptor 3-dependent inflammation after skin injury. Nat Med 15:1377–1382. https://doi.org/10.1038/nm.2062
13. Bataille A, Lee-Cruz L, Tripathi B, Kim H, Waldman B. 2016. Microbiome variation across amphibian skin regions: implications for chytridiomycosis mitigation efforts. Microb Ecol 71:221–232. https://doi.org/10.1007/s00248-015-0653-0
14. Belden LK, Harris RN. 2007. Infectious diseases in wildlife: the community ecology context. Frontiers in Ecology and the Environment 5:533–539. https://doi.org/10.1890/060122
15. Harris RN, James TY, Lauer A, Simon MA, Patel A. 2006. Amphibian pathogen *Batrachochytrium dendrobatidis* is inhibited by the cutaneous bacteria of amphibian species. EcoHealth 3:53–56. https://doi.org/10.1007/s10393-005-0009-1
16. Woodhams DC, Ardipradja K, Alford RA, Marantelli G, Reinert LK, Rollins-Smith LA. 2007. Resistance to chytridiomycosis varies among amphibian species and is correlated with skin peptide defenses. Ani Cons 10:409–417. https://doi.org/10.1111/j.1469-1795.2007.00130.x
17. Bates KA, Clare FC, O'Hanlon S, Bosch J, Brookes L, Hopkins K, McLaughlin EJ, Daniel O, Garner TWJ, Fisher MC, Harrison XA. 2018. Amphibian chytridiomycosis outbreak dynamics are linked with host skin bacterial community structure. Nat Commun 9:693. https://doi.org/10.1038/s41467-018-02967-w
18. Jani AJ, Briggs CJ. 2014. The pathogen *Batrachochytrium dendrobatidis* disturbs the frog skin microbiome during a natural epidemic and experimental infection. Proc Natl Acad Sci U S A 111:E5049–58. https://doi.org/10.1073/pnas.1412752111
19. Allender MC, Baker S, Britton M, Kent AD. 2018. Snake fungal disease alters skin bacterial and fungal diversity in an endangered rattlesnake. Sci Rep 8:12147. https://doi.org/10.1038/s41598-018-30709-x
20. Lloyd MM, Pespeni MH. 2018. Microbiome shifts with onset and progression of sea star wasting disease revealed through time course sampling. Sci Rep 8:16476. https://doi.org/10.1038/s41598-018-34697-w
21. Blehert DS, Hicks AC, Behr M, Meteyer CU, Berlowski-Zier BM, Buckles EL, Coleman JTH, Darling SR, Gargas A, Niver R, Okoniewski JC, Rudd RJ, Stone WB. 2009. Bat white-nose syndrome: an emerging fungal pathogen Science 323:227. https://doi.org/10.1126/science.1163874
22. Lorch J. M., Meteyer CU, Behr MJ, Boyles JG, Cryan PM, Hicks AC, Ballmann AE, Coleman JTH, Redell DN, Reeder DM, Blehert DS. 2011. Experimental infection of bats with *Geomyces destructans* causes white-nose syndrome. Nature 480:376–378. https://doi.org/10.1038/nature10590
23. Warnecke L, Turner JM, Bollinger TK, Lorch JM, Misra V, Cryan PM, Wibbelt G, Blehert DS, Willis CKR. 2012. Inoculation of bats with European *Geomyces destructans* supports the novel pathogen hypothesis for the origin of white-nose syndrome. Proc Natl Acad Sci U S A 109:6999–7003. https://doi.org/10.1073/pnas.1200374109
24. Meteyer CU, Buckles EL, Blehert DS, Hicks AC, Green DE, Shearn-Bochsler V, Thomas NJ, Gargas A, Behr MJ. 2009. Histopathologic criteria to confirm white-nose syndrome in bats. J Vet Diagn Invest 21:411–414. https://doi.org/10.1177/104063870902100401
25. Verant ML, Meteyer CU, Speakman JR, Cryan PM, Lorch JM, Blehert DS. 2014. White-nose syndrome initiates a cascade of physiologic disturbances in the hibernating bat host. BMC Physiol. 14:10. https://doi.org/10.1186/s12899-014-0010-4
26. Warnecke L, Turner JM, Bollinger TK, Misra V, Cryan PM, Blehert DS, Wibbelt G, Willis CKR. 2013. Pathophysiology of white-nose syndrome in bats: a mechanistic model linking wing damage to mortality. Biol Lett 9:20130177. https://doi.org/10.1098/rsbl.2013.0177
27. Frick WF, Pollock JF, Hicks AC, Langwig KE, Reynolds DS, Turner GG, Butchkoski CM, Kunz TH. 2010. An emerging disease causes regional population collapse of a common North American bat species. Science 329:679–682. https://doi.org/10.1126/science.1188594
28. Frick WF, Puechmaille SJ, Hoyt JR, Nickel KE, Langwig JT, Foster KE, Barlow T, Bartonička D. 2015. Disease alters macroecological patterns of

North American bats. Glob Ecol Biogeogr 24:741–749. https://doi.org/10.1111/geb.12290
29. Langwig KE, Frick WF, Bried JT, Hicks AC, Kunz TH, Kilpatrick AM. 2012. Sociality, density-dependence and microclimates determine the persistence of populations suffering from a novel fungal disease, white-nose syndrome. Ecol Lett 15:1050–1057. https://doi.org/10.1111/j.1461-0248.2012.01829.x
30. Langwig KE, Hoyt JR, Parise KL, Frick WF, Foster JT, Kilpatrick AM. 2017. Resistance in persisting bat populations after white-nose syndrome invasion. Philos Trans R Soc Lond B Biol Sci 372:20160044. https://doi.org/10.1098/rstb.2016.0044
31. Langwig KE, Hoyt JR, Parise KL, Kath J, Kirk D, Frick WF, Foster JT, Kilpatrick AM. 2015b. Invasion dynamics of white-nose syndrome fungus, midwestern United States, 2012-2014. Emerg Infect Dis 21:1023–1026. https://doi.org/10.3201/eid2106.150123
32. Frick WF, Cheng TL, Langwig KE, Hoyt JR, Janicki AF, Parise KL, Foster JT, Kilpatrick AM. 2017. Pathogen dynamics during invasion and establishment of white-nose syndrome explain mechanisms of host persistence. Ecology 98:624–631. https://doi.org/10.1002/ecy.1706
33. Reichard JD, Fuller NW, Bennett AB, Darling SR, Moore MS, Langwig KE, Preston ED, von Oettingen S, Richardson CS, Reynolds DS. 2014. Interannual survival of *Myotis lucifugus* (Chiroptera: vespertilionidae) near the epicenter of white-nose syndrome. Northeast Nat (Steuben) 21:N56–N59. https://doi.org/10.1656/045.021.0410
34. Langwig, K. E., W. F. Frick, R. Reynolds, K. L. Parise, K. P. Drees, J. R. Hoyt, T. L. Cheng, T. H. Kunz, J. T. Foster, and A. M. Kilpatrick. 2015a. Host and pathogen ecology drive the seasonal dynamics of a fungal disease, white-nose syndrome. Proceedings of the Royal Society. Biological sciences 282:20142335.
35. Meteyer CU, Valent M, Kashmer J, Buckles EL, Lorch JM, Blehert DS, Lollar A, Berndt D, Wheeler E, White CL, Ballmann AE. 2011. Recovery of little brown bats (*Myotis lucifugus*) from natural infection with *Geomyces destructans*, white-nose syndrome. J Wildl Dis 47:618–626. https://doi.org/10.7589/0090-3558-47.3.618
36. Hoyt J. R., Langwig KE, Okoniewski J, Frick WF, Stone WB, Kilpatrick AM. 2015. Long-term persistence of *Pseudogymnoascus destructans*, the causative agent of white-nose syndrome, in the absence of bats. Ecohealth 12:330–333. https://doi.org/10.1007/s10393-014-0981-4
37. Lorch Jeffrey M, Muller LK, Russell RE, O'Connor M, Lindner DL, Blehert DS. 2013. Distribution and environmental persistence of the causative agent of white-nose syndrome, *Geomyces destructans*, in bat Hibernacula of the eastern United States. Appl Environ Microbiol 79:1293–1301. https://doi.org/10.1128/AEM.02939-12
38. Hoyt Joseph R., Kilpatrick AM, Langwig KE. 2021. Ecology and impacts of white-nose syndrome on bats. Nat Rev Microbiol 19:196–210. https://doi.org/10.1038/s41579-020-00493-5
39. Langwig KE, Frick WF, Hoyt JR, Parise KL, Drees KP, Kunz TH, Foster JT, Kilpatrick AM. 2016. Drivers of variation in species impacts for a multi-host fungal disease of bats. Philos Trans R Soc Lond B Biol Sci 371:20150456. https://doi.org/10.1098/rstb.2015.0456
40. Avena CV, Parfrey LW, Leff JW, Archer HM, Frick WF, Langwig KE, Kilpatrick AM, Powers KE, Foster JT, McKenzie VJ. 2016. Deconstructing the bat skin microbiome: influences of the host and the environment. Front Microbiol 7:1753. https://doi.org/10.3389/fmicb.2016.01753
41. Forsythe A, Fontaine N, Bissonnette J, Hayashi B, Insuk C, Ghosh S, Kam G, Wong A, Lausen C, Xu J, Cheeptham N. 2022. Microbial isolates with anti-*Pseudogymnoascus destructans* activities from Western Canadian bat wings. Sci Rep 12:9895. https://doi.org/10.1038/s41598-022-14223-9
42. Lemieux-Labonté V., Simard A, Willis CKR, Lapointe F-J. 2017. Enrichment of beneficial bacteria in the skin microbiota of bats persisting with white-nose syndrome. Microbiome 5:115. https://doi.org/10.1186/s40168-017-0334-y
43. Lemieux-Labonté Virginie, Dorville NAS-Y, Willis CKR, Lapointe F-J. 2020. Antifungal potential of the skin microbiota of hibernating big brown bats (*Eptesicus fuscus*) infected with the causal agent of white-nose syndrome. Front Microbiol 11:588889. https://doi.org/10.3389/fmicb.2020.588889
44. Vanderwolf KJ, Campbell LJ, Taylor DR, Goldberg TL, Blehert DS, Lorch JM. 2021. Mycobiome traits associated with disease tolerance predict many Western North American bat species will be susceptible to white-nose syndrome. Microbiol Spectr 9:e0025421. https://doi.org/10.1128/Spectrum.00254-21
45. Winter AS, Hathaway JJM, Kimble JC, Buecher DC, Valdez EW, Porras-Alfaro A, Young JM, Read KJH, Northup DE. 2017. Skin and fur bacterial diversity and community structure on American Southwestern bats: effects of habitat, geography and bat traits. PeerJ 5:e3944. https://doi.org/10.7717/peerj.3944
46. Cogen AL, Nizet V, Gallo RL. 2008. Skin microbiota: a source of disease or defence? Br J Dermatol 158:442–455. https://doi.org/10.1111/j.1365-2133.2008.08437.x
47. Shuey MM, Drees KP, Lindner DL, Keim P, Foster JT. 2014. Highly sensitive quantitative PCR for the detection and differentiation of *Pseudogymnoascus Destructans* and other *Pseudogymnoascus* species. Appl Environ Microbiol 80:1726–1731. https://doi.org/10.1128/AEM.02897-13
48. Muller LK, Lorch JM, Lindner DL, O'Connor M, Gargas A, Blehert DS. 2013. Bat white-nose syndrome: a real-time TaqMan polymerase chain reaction test targeting the Intergenic spacer region of *Geomyces destructans*. Mycologia 105:253–259. https://doi.org/10.3852/12-242
49. Janicki AF, Frick WF, Kilpatrick AM, Parise KL, Foster JT, McCracken GF. 2015. Efficacy of visual surveys for white-nose syndrome at bat hibernacula. PLoS One 10:e0133390. https://doi.org/10.1371/journal.pone.0133390
50. Huebschman JJ, Hoerner SA, White JP, Kaarakka HM, Parise KL, Foster JT. 2019. Detection of *Pseudogymnoascus destructans* on wisconsin bats during summer. J Wildl Dis 55:673–677. https://doi.org/10.7589/2018-06-146
51. Caporaso JG, Lauber CL, Walters WA, Berg-Lyons D, Huntley J, Fierer N, Owens SM, Betley J, Fraser L, Bauer M, Gormley N, Gilbert JA, Smith G, Knight R. 2012. Ultra-high-throughput microbial community analysis on the Illumina Hiseq and Miseq platforms. ISME J 6:1621–1624. https://doi.org/10.1038/ismej.2012.8
52. Martin M. 2011. Cutadapt removes adapter sequences from high-throughput sequencing reads. EMBnet j 17:10. https://doi.org/10.14806/ej.17.1.200
53. Knight R, Vrbanac A, Taylor BC, Aksenov A, Callewaert C, Debelius J, Gonzalez A, Kosciolek T, McCall L-I, McDonald D, Melnik AV, Morton JT, Navas J, Quinn RA, Sanders JG, Swafford AD, Thompson LR, Tripathi A, Xu ZZ, Zaneveld JR, Zhu Q, Caporaso JG, Dorrestein PC. 2018. Best practices for analysing microbiomes. Nat Rev Microbiol 16:410–422. https://doi.org/10.1038/s41579-018-0029-9
54. Salter SJ, Cox MJ, Turek EM, Calus ST, Cookson WO, Moffatt MF, Turner P, Parkhill J, Loman NJ, Walker AW. 2014. Reagent and laboratory contamination can critically impact sequence-based microbiome analyses. BMC Biol. 12:87. https://doi.org/10.1186/s12915-014-0087-z
55. Katoh K, Standley DM. 2013. MAFFT multiple sequence alignment software version 7: improvements in performance and usability. Mol Biol Evol 30:772–780. https://doi.org/10.1093/molbev/mst010
56. Price MN, Dehal PS, Arkin AP. 2010. FastTree 2--approximately maximum-likelihood trees for large alignments. PLoS One 5:e9490. https://doi.org/10.1371/journal.pone.0009490
57. Anderson MJ, Walsh DCI. 2013. PERMANOVA, ANOSIM, and the mantel test in the face of heterogeneous dispersions: what null hypothesis are you testing. Ecol Mon 83:557–574. https://doi.org/10.1890/12-2010.1
58. Andam CP, Doroghazi JR, Campbell AN, Kelly PJ, Choudoir MJ, Buckley DH. 2016. A latitudinal diversity gradient in terrestrial bacteria of the genus *Streptomyces*. mBio 7:e02200-15. https://doi.org/10.1128/mBio.02200-15
59. Segata N, Izard J, Waldron L, Gevers D, Miropolsky L, Garrett WS, Huttenhower C. 2011. Metagenomic biomarker discovery and explanation. Genome Biol. 12:R60. https://doi.org/10.1186/gb-2011-12-6-r60
60. Platas G, Morón R, González I, Collado J, Genilloud O, Peláez F, Diez MT. 1998. Production of antibacterial activities by members of the family pseudonocardiaceae: influence of nutrients. World J Microbiol Biotechnol 14:521–527. https://doi.org/10.1023/A:1008874203344
61. Currie CR, Scott JA, Summerbell RC, Malloch D. 1999. Fungus-growing ants use antibiotic-producing bacteria to control garden parasites. Nature 398:701–704. https://doi.org/10.1038/19519

62. Cafaro MJ, Currie CR. 2005. Phylogenetic analysis of mutualistic filamentous bacteria associated with fungus-growing ants. Can J Microbiol 51:441–446. https://doi.org/10.1139/w05-023
63. Currie CR, Poulsen M, Mendenhall J, Boomsma JJ, Billen J. 2006. Coevolved crypts and exocrine glands support mutualistic bacteria in fungus-growing ants. Science 311:81–83. https://doi.org/10.1126/science.1119744
64. Bergey, D. H. 1989. Bergey's Manual of Systematic Bacteriology. Williams & Wilkins.
65. Bowman SM, Free SJ. 2006. The structure and synthesis of the fungal cell wall. Bioessays 28:799–808. https://doi.org/10.1002/bies.20441
66. Kong HH, Segre JA. 2012. Skin microbiome: looking back to move forward. J Invest Dermatol 132:933–939. https://doi.org/10.1038/jid.2011.417
67. Vanderwolf K, Malloch D, McAlpine D, New Brunswick Museum. 2015. Fungi on white-nose infected bats (*Myotis* spp.) in Eastern Canada show no decline in diversity associated with *Pseudogymnoascus destructans* (Ascomycota: Pseudeurotiaceae). IJS 45:43–50. https://doi.org/10.5038/1827-806X.45.1.1946
68. Holz PH, Lumsden LF, Marenda MS, Browning GF, Hufschmid J, Baker ML. 2018. Two subspecies of bent-winged bats (*Miniopterus orianae bassanii and oceanensis*) in Southern Australia have diverse fungal skin flora but not *Pseudogymnoascus destructans*. PLoS ONE 13:e0204282. https://doi.org/10.1371/journal.pone.0204282
69. Lorch J. M., Minnis AM, Meteyer CU, Redell JA, White JP, Kaarakka HM, Muller LK, Lindner DL, Verant ML, Shearn-Bochsler V, Blehert DS. 2015. The fungus *Trichophyton redellii* sp. nov. causes skin infections that resemble white-nose syndrome of hibernating bats. J Wildl Dis 51:36–47. https://doi.org/10.7589/2014-05-134
70. Palmer JM, Drees KP, Foster JT, Lindner DL. 2018. Extreme sensitivity to ultraviolet light in the fungal pathogen causing white-nose syndrome of bats. Nat Commun 9:35. https://doi.org/10.1038/s41467-017-02441-z